From molten salts to ionic liquids: effect of ion asymmetry and charge distribution

2008 J. Phys.: Condens. Matter 20 035108

(http://iopscience.iop.org/0953-8984/20/3/035108)

IOP Publishing Journal of Physics: Condensed Matter

J. Phys.: Condens. Matter **20** (2008) 035108 (9pp) doi:10.1088/0953-8984/20/03/035108

From molten salts to ionic liquids: effect of ion asymmetry and charge distribution

Marco Malvaldi[1] **and Cinzia Chiappe**

Dipartimento di Chimica Bioorganica e Biofarmacia, Università degli Studi di Pisa,
Via Bonanno Pisano 33, 56126 Pisa, Italy

E-mail: marco@dcci.unipi.it

Received 24 August 2007, in final form 15 October 2007
Published 17 December 2007
Online at stacks.iop.org/JPhysCM/20/035108

Abstract

We studied the influence of ion shape asymmetry and charge distribution on the liquid structure and transport properties of ionic liquids by the molecular dynamics of schematic models. The ion structure asymmetry results in a less compact packing, while the charge distribution gives potential wells with reduced depth with respect to the single-site centred charges. Both these aspects contribute to accelerate the dynamics of the melt. The liquids display a clearly detectable supercooled region, in which two different liquid structures appear to be present contemporarily. The diffusion process, as usual in supercooled liquids, proceeds through a cage-escaping process; the diffusion constants nevertheless show an opposite behaviour with respect to expectations from the cavity size distribution. The observed transient liquid structure can help to explain some surprising features of the diffusive behaviour of these systems.

(Some figures in this article are in colour only in the electronic version)

1. Introduction

In the last decade, a classical subject of physics such as the structure and dynamics of molten salts, e.g. liquids constituted solely by ions, has attracted a considerable amount of interest. One of the main driving forces for such interest is given by the fascinating possibilities that particular kinds of molten salts, named room-temperature ionic liquids (RTILs), have opened to physics and chemistry [1, 2].

Despite all the positive characteristics making ionic liquids and RTILs promising media for organic synthesis and a possible basis for advanced materials [3], there is still a lack of knowledge about the origin of their thermodynamic and transport properties. Among the various issues needing a deeper or more complete understanding, there are the transport properties, such as viscosity or bulk conductivity, the ionic diffusion coefficient, and the extent of ion association. In addition, such materials often show a marked deviation from the ideal relations of mass and charge transport in liquids, such as the Nernst–Einstein and the Stokes–Einstein equation. The molecular simulation techniques are, in principle, very useful for studying unusual features of transport properties, and several molecular dynamics works [4–10] have been published up to now.

Because ionic liquids have complex molecular structure, the correlation of the properties displayed by these materials to their structure may be very complicated; there is then a need to rationalize the behaviour of this class of liquids in a general picture, which is able to keep track of their essential characteristics. With this aim, the development of a simple and reliable coarse-grained model retaining only the essential features of RTILs and able to reproduce their properties would greatly help the scientific investigation of these systems.

In the past, research on complex liquids has gained a lot through the development of coarse-grained models with a very low level of complexity such as the bond fluctuation model for polymers [11], retaining only chain uncrossability, the Gay–Berne model for liquid crystals [12], which assimilated the mesogenic molecule to a prolate ellipsoid, and the soft primitive model (SPM) for the study of the structure of ionic fluids [13]. Simulations of these simple models generally showed agreement with experimental trends, and in some cases useful predictions have been possible on the basis of their results.

Our main purpose is to understand to what extent basic changes in the gross electronic and molecular structure of the ions, without changing their total charge, can affect the

[1] Author to whom any correspondence should be addressed.

macroscopic behaviour of such systems. It is known, for example, that size asymmetry alone has a noticeable effect on the phase diagram of ionic liquids [14, 15] and on their surface tension [16].

In this work, we investigate the influence of ion structure asymmetry (ions consisting of a different number of sites) and of the spreading of charge on the ion sites on the structure and dynamics of a molten salt. Our results show that the liquid structure, the onset of the supercooling regime and the overall dynamics of the ionic melt are deeply affected by these aspects.

2. Model system and simulation details

2.1. Model setup

At the present time, the most investigated ionic liquids are composed of a 1,3 di-substituted imidazolium cation, bearing short alkyl chains (ethyl–butyl typically) and an inorganic anion. For these, the main contribution to intermolecular energy is given by the Coulomb term, and the strength of other intermolecular terms is usually much lower (it can be about one order of magnitude less [8]); this clear separation of energies allows us to imagine that a simple model, in which the leading role is played by the charge distribution, can reproduce most essential features of ionic liquid. Recently, it has been shown that ionic liquids in which one of the constituents (typically the cation) contains a moderately long alkyl chain have a non-negligible contribution of dispersion terms to the interaction energy, sometimes of the same order of magnitude as the Coulombic contribution [17]. Nevertheless, in this preliminary analysis we will not take into account the effect of dispersion (except for its contribution to repulsive forces) which could be added in a second stage.

We do not intend to build a model able to represent the essential features of all the possible room-temperature ionic liquids; rather, following the route by which a monovalent molten salt can be transformed in a ionic liquid, we pursue two objectives. The first is, as has been said, to understand the relative extent that the electronic and molecular structure can have on the bulk structure and dynamic properties of these systems. The second is to clarify which aspects of molten salts and ionic liquids are to be expected on the basis of their primary nature of liquids composed of charged species, without the need to invoke specific chemical interactions (such as hydrogen bonding) to explain their presence.

The peculiarities that we believe to be fundamental, at a molecular level, in a low-temperature melting ionic liquid are the following:

(1) The two ions have consistently different sizes (usually the cation is larger than the anion) and different symmetry and geometrical shape, the cation being (usually) far from a spherical shape, while the anion often (at least, in first-generation ionic liquids) retains some spherical character through the retention of one or more operations of spherical symmetry, as in Cl– , $AlCl_4$–, SbF_4–, BF_4–, PF_6–.

(2) The net positive or negative charge is not centred at a single site, but is distributed over the different building blocks.

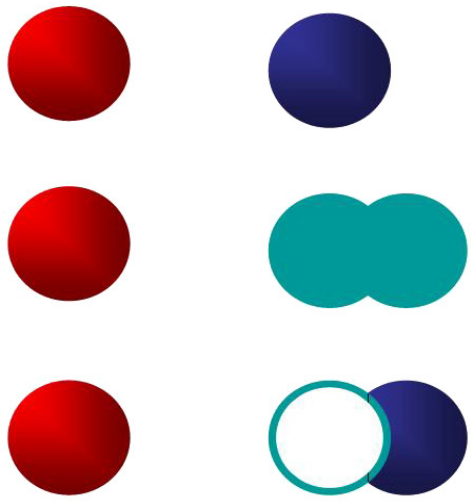

Figure 1. Schematic representation of the three systems studied: system M (top), system A (middle), system B (bottom).

(3) The n-dimensional potential energy surface of interaction between the two oppositely charged ions displays several essentially degenerate energy minima; at a finite temperature, the anion has different accessible positions towards the cation, while others are strongly unfavourable [18, 19]. This aspect is (partially) a consequence of points (1) and (2).

To describe briefly the consequences that are expected from such peculiarities, we point out that the different size of the ions, together with the complex and unsymmetrical molecular shape of at least one of the ions, will result in a poor packing ability at low temperatures, thus lowering the binding energy of the solid or glassy state and giving a lower liquid-to-solid transition temperature with respect to an ionic system composed of spherical ions of equivalent or similar size [20].

The spreading of charge distribution is, similarly, expected to give rise to potential energy wells with a reduced depth (compared with the interaction of two single-site charges) due to the lower strength of the Coulomb interactions for most of the anion–cation mutual arrangements.

Finally, the presence of multiple potential energy minima for the ion pairing geometry can result in a polymorphic structure of the solid or the glass and in the presence of static and dynamic heterogeneities in the liquid state [21, 22]. On the other hand, the presence of orientational order induced by the combination of attraction (including specific attraction, such as hydrogen bonding) and short-range repulsion can result in a non-negligible degree of structural ordering even in the liquid state [23].

In order to retain the features indicated above, but still retain a very simple model, we represent our model ionic liquid as a cation formed by two sites, bounded by an harmonic bond, and a single-site anion (see figure 1). In the following, all energies, lengths, charges and times are given in reduced units. The site–site interaction energy for ions belonging to

two different molecules is given by:

$$U_{\text{tot}} = \sum_{i,j} U_{\text{LJ}}(r_{ij}) + U_{\text{Coulomb}}(r_{ij}) \quad (1)$$

where

$$U_{\text{LJ}}(r_{ij}) = \left[4\varepsilon_{ij}\left(\left(\frac{\sigma_{ij}}{r_{ij}}\right)^{12} - \left(\frac{\sigma_{ij}}{r_{ij}}\right)^{6}\right)\right]\theta\left(r_{\text{cut}} - r_{ij}\right) \quad (2)$$

is the usual truncated-and-shifted Lennard-Jones (LJ) potential, providing the repulsive contribution, and

$$U_{\text{Coulomb}}(r_{ij}) = \frac{q_i q_j}{r_{ij}} \quad (3)$$

is the Coulombic contribution. Here σ_{ij} is the Lennard-Jones diameter, ε_{ij} is the interaction energy and $\theta(r)$ is the Heaviside function, leading to zero Lennard-Jones contribution for $r_{\text{cut}} - r_{ij} < 0$. The cutoff energy in equation (2) is chosen to set the value of the interaction energy to zero at the cutoff value.

In this model the parameters of the LJ interaction have been set, independently of the nature of the site, to unity value in reduced units ($\sigma_{ij} = 1$, $\varepsilon_{ij} = 1$ $\forall i, j$). The cutoff was positioned at $r_{\text{cut}} = \sqrt[6]{2}$, in order to ensure that the Lennard-Jones contribution is only repulsive. The sites in the cation were bounded together by an harmonic force of potential $U_{\text{bond}} = 100.0kT$, with an equilibrium value of $r_{\text{eq}} = 0.8\sigma$. The harmonic force was the only one acting between bounded sites (intermolecular contributions were switched off between sites belonging to the same molecule). Both the anion and the cation were assigned a total reduced mass $m = 1$.

For the value of the charges, two different choices were made: in the first system (system A) an equivalent charge of value $q_+ = 5.0$ was placed on both sites of the cation, while in the second system (system B) a single charge of value $q_+ = 10.0$ was placed on one of the sites of the cation, leaving the remaining one neutral. In both systems, a charge of value $q_- = -10.0$ was placed on the single-site anion. The long-range contribution of the charges on the potential energy was evaluated by Ewald summation, with $\alpha = 5.6$ and $n_k = 5$. For comparison, an equivalent model built with a single-site cation with charge $q_+ = 10.0$ (system M, representing a monovalent molten salt) has been studied. To have a rapid comparison with SI units, choosing a unit mass of 50.0 amu, a unit energy $\varepsilon = 4.18605$ kJ mol^{-1} and a unit length $\sigma = 0.333$ nm gives a unit temperature $T = 503.46$ K and a unit time $t = 1.14$ ps. With this choice of reduced unit values, a unit valence charge (a charge of one electron) corresponds to a reduced charge of 10.0. Our system is thus composed of cations and anions of total charge ± 1 in terms of electron charge. The values of the parameter chosen gave an equilibrium distance of $r_{\text{eq}} = 0.8$ for the cation intersite bond length distance and $r_{\text{eq}} = 0.92$ (0.95) for the intersite LJ + Coulomb potential between differently charged sites for system B (system A), respectively; this difference in intramolecular and intermolecular length scales was chosen to prevent possible crystallization. A pictorial representation of the three models is presented in figure 1.

The systems have been simulated in the *NPT* ensemble at $P = 1$, corresponding to a pressure of 1908.95 atm in SI units; even if such a pressure is quite high with respect to the ambient pressure, the qualitative aspects of ionic liquids should not be affected by a pressure shift, especially for what concerns dynamics [24]. Nevertheless, since this work proposes a coarse-grained model, our main interest is to present the capabilities of such a model rather than reproducing experimental data.

2.2. Simulation details

All the calculations were performed with the software COGNAC 5, distributed in the platform OCTA 2005 [25].

For each system, composed of 500 ionic pairs, a starting random configuration has been equilibrated at the reduced temperature 5 T in the *NPT* ensemble with the Andersen–Nose–Hoover thermobarostat (with a thermal coupling constant and cell mass of $Q = 20.0$ and $M = 50.0$, respectively) for $t = 100.0$ with a time step of $\delta t = 0.001$; then a production run in the *NVE* ensemble was performed. For each temperature, the system was obtained by subsequent cooling from the immediate upper temperature; starting from the last configuration, the new temperature was switched on and the system allowed to relax in the *NPT* ensemble until equilibration was reached. A production run in the *NVE* ensemble was then performed.

3. Results

3.1. Liquid structure

A significant measurement of local ordering in the fluid can be given by understanding the relative alignment of the cation with respect to the anion. To get a deeper insight into the structural order of these systems, we defined an orientational order parameter relating the mutual arrangement of the cation and the anion, $q_\alpha = \cos\theta_{i\alpha}$, where, for each pair of anion–cation sites directly bounded (that is, with a distance less than the first minimum in $g(r)_{+-}$), $\theta_{i\alpha}$ is the angle formed by the vector $\vec{i}$ joining the nearest (bounded) site of the cation and the anion, and the vector $\vec{\alpha}$ joining the same bounded site to the other site of the cation. A pictorial representation of these vectors is given in figure 2. The probability distribution of this orientational order parameter (figure 3) clearly shows the rise of orientational short-range order as the system is cooled; the function for system A shows two distinct maxima at the values corresponding to the structures schematically reported in figure 2.

A third structure, characterized by the neutral site as the first neighbour in the solvation shell, arises in system B. It must be observed that such preferential structures arise only from packing necessities, and are not merely a consequence of specific ionic pair directional interactions, and thus could not be inferred simply by inspection of the pair potential. The progressive rise of the height of peaks in $f(q)$ suggests the formation of aggregates of growing dimensions, or an enhancement of the number of aggregates, as the temperature decreases; anyway, the areas pertaining to the two peaks

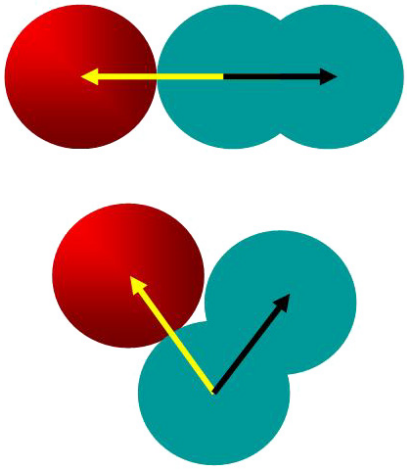

Figure 2. Two-dimensional representation of possible packing structures of cation molecules (blue) around an anion (red). The structure on the bottom, corresponding to positive value of $\cos\theta$, is the prevailing structure in the whole range of temperatures studied, while the structure on the top is revealed detectably only approaching the glass transition from the liquid state. A pictorial representation of the vectors defining the angle θ as the angle formed by the vector i (left-directed, yellow) and the vector α (right-directed, black) is given.

show different relative growth as the temperature is lowered. This is particularly evident from system B, where the growth of the peak given by the first structure ($\cos\theta = -1$) is almost undetectable. Such a bimodal distribution and its inhomogeneous growth with cooling suggests the presence of more than one liquid structure in the bulk liquid; this 'structural heterogeneity' feature has been recognized by computer simulations in ionic liquids [26, 22] and in other polar liquids, like supercooled water [23, 27]. This aspect implies that the transient arrangement of the cations surrounding an anion follows two preferential structured paths, with different relative probabilities. As we will show later, in agreement with the observation previously made by Hu and Margulis on realistic systems [21], such structural heterogeneities consistently affect the dynamics.

3.2. Supercooling regime

The peculiar property of RTILs is, as the name suggests, the low temperatures at which they can be cooled without freezing, but instead remaining in the liquid state, if compared to ordinary (inorganic) molten salts such as, for example, alkali halides. A physically sound qualitative picture can explain this phenomenon in terms of the charge distribution on bulky and large ions and on the usually different size and structures of the anion and the cation, frustrating an efficient packing and then lowering the liquid–glass transition. Nevertheless, a deeper analysis of such a dependence can be afforded with a coarse-grained model in which all the molecular parameters characterizing the system can be varied by choice, so that a wide and well-sampled ensemble of case studies can be planned.

The supercooled behaviour in liquids is given by a deviation from the thermodynamic equilibrium of the system,

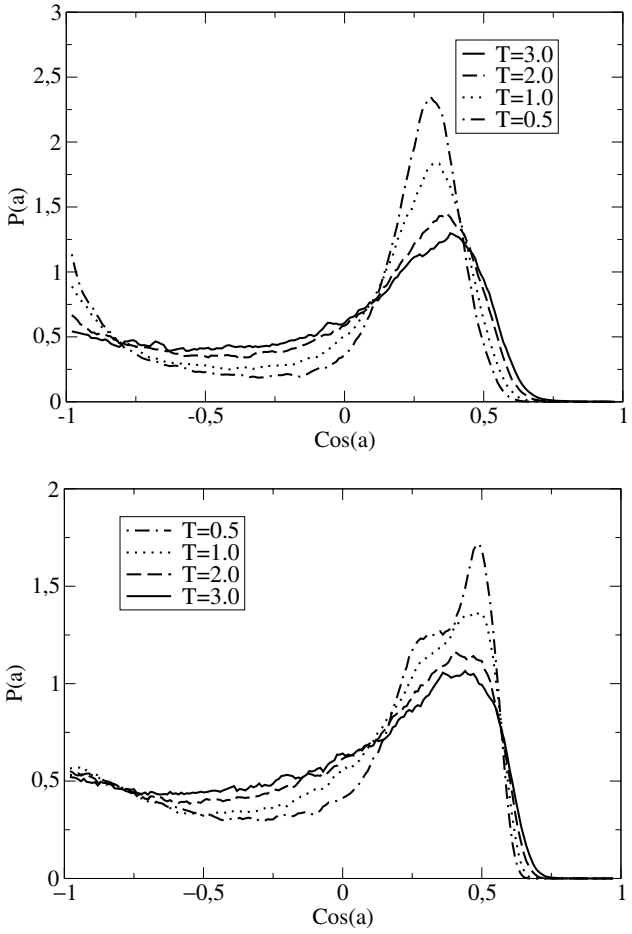

Figure 3. Population $f(q)$ versus the order parameter $q = \langle\cos\theta_{ij}\rangle$ (defined in section 3.1) for system A (top) and system B (bottom) at growing temperatures. See figure 2 for a definition of the angle θ_{ij}.

and in this regime the thermodynamic state functions depend on the length of the simulation; for this reason, the onset of such behaviour (which is strongly dependent on the conditions of the simulation) cannot be defined unequivocally. Usually, this onset is studied by monitoring a structural quantity as a function of temperature and detecting a sharp deviation in its behaviour [28].

The onset of supercooling has been studied by progressively cooling the system from the starting temperature $T = 5.0$, and calculating the number of neighbours in the first solvation shell of the anion for each temperature; plotting this data against temperature, as reported in figure 4, two regions (liquid and supercooled) can be identified due to the different steepness of the function. The onset of the supercooled region occurs at different temperatures, at $T = 3.26$ for system M, $T = 2.81$ for the system with localized charge (system B), and $T = 2.44$ for the system with distributed charge (system A).

The systems with the dimeric cation have been analysed further by calculating the orientational correlation function of the internuclear axis of the cation,

$$\Omega(t) = \sum_i \frac{\langle \vec{r}_i(t)\vec{r}_i(0)\rangle}{\langle \vec{r}_i(0)\vec{r}_i(0)\rangle}. \qquad (4)$$

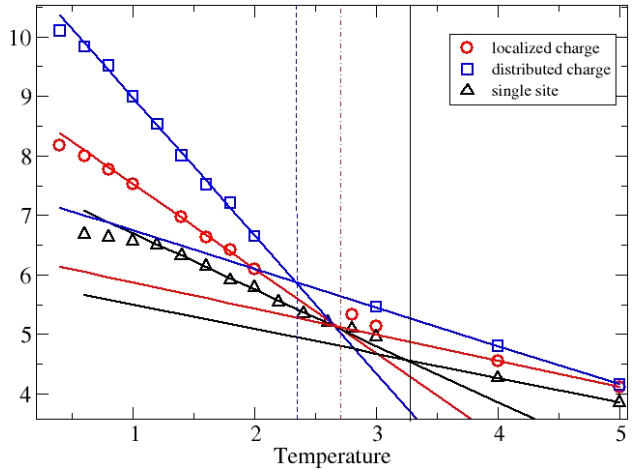

Figure 4. Average number of neighbours for the anion versus temperature for system A (blue squares), system B (red circles), and system M (black triangles). The straight lines mark the onset of the supercooling regime for the three systems.

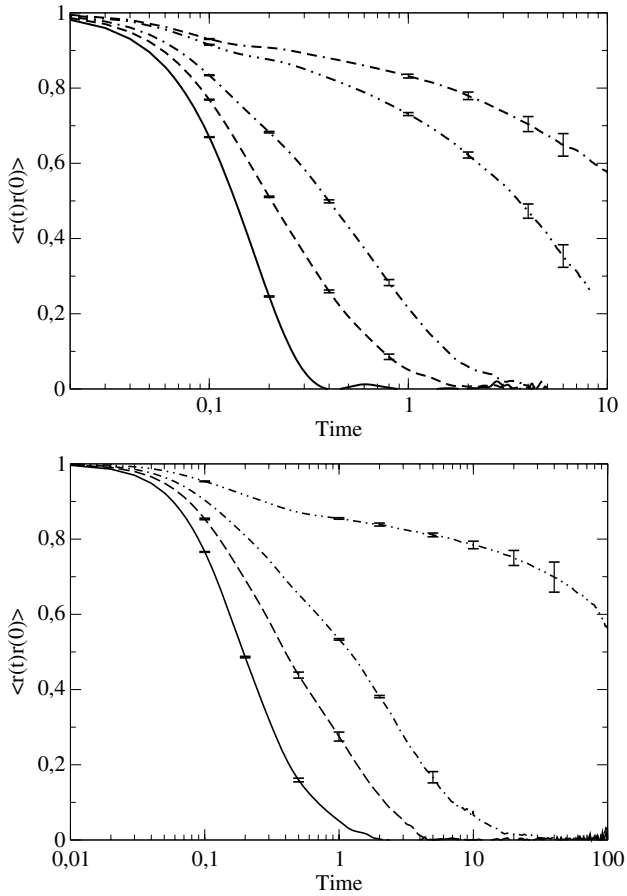

Figure 5. Top: internuclear vector correlation function at temperatures $T = 5.0$ (full), 3.0 (dashed), 2.0 (dashed–dotted), 1.0 (dashed–double dotted), 0.8 (double dashed–dotted) for system A. Bottom: internuclear vector correlation function at temperatures $T = 5.0$ (full), 3.0 (dashed), 2.0 (dashed–dotted), 1.0 (dashed–double dotted).

As can be observed in figure 5, the correlation of the rotational motion shows a single decay for the liquid, while in the supercooled phase a two-step decay is present. Such

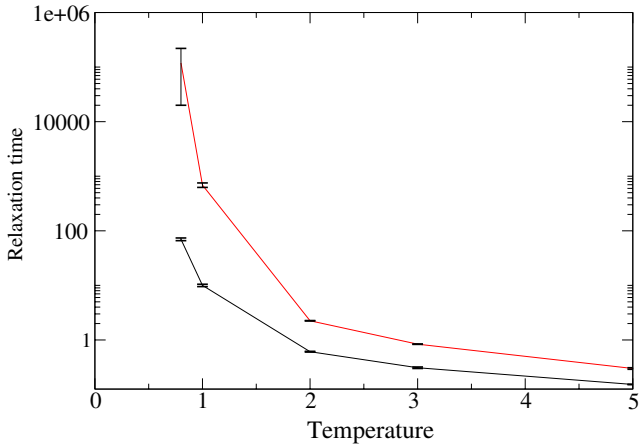

Figure 6. Relaxation times of the internuclear vector autocorrelation function for the system with distributed charge (system A, circles) and for the system with localized charge (system B, squares). The times have been obtained by fitting the correlation functions with a single exponential ($T = 5.0$, 3.0) or with a double exponential ($T = 2.0$, 1.0, 0.8; in this case, the longest relaxation time is presented).

behaviour can be explained by assuming that cations librate in a cage given by an aggregate with long relaxation time; the fast (and incomplete) relaxation of the internuclear vector orientation is thus given by the libration motion, while the orientation is completely relaxed only by the slow disruption of the aggregate. A similar behaviour has already been observed in ionic liquids [8, 21, 29].

The orientational relaxation times have been obtained by fitting the orientational correlation function with a double exponential function,

$$f(t) = a \exp[-t/\tau_\beta] + (1 - a) \exp[-t/\tau_\alpha]. \qquad (5)$$

In figure 6 the orientational relaxation times for the slow process, τ_α, for the cation intramolecular vector are reported as a function of temperature for the systems studied. We are aware of the fact that in supercooled systems a strong deviation from exponentiality of the relaxation behaviour is expected; nevertheless, since for some systems we could not obtain a complete relaxation of the correlation function on the timescale of the simulation, and because our purpose in this analysis is to obtain a qualitative trend of relaxation times, we felt that the analysis of the non-exponentiality parameters would not have been meaningful in this work.

The glass transition temperatures can be obtained qualitatively, in order to compare the temperature at which a structural arrest is expected for the various systems, on the basis of the dynamics of the system; it must be borne in mind, however, that the temperature that is obtained is dependent on the kind of measurement performed (that is, on the molecular motion probed) by the very nature of the transition. Usually, the dynamic glass transition temperature (by an empirical kinetic definition) is defined as the temperature at which the system reaches a relaxation time of 100 s [31]. Extrapolating the relaxation times by fitting them with a Vogel–Fulcher law,

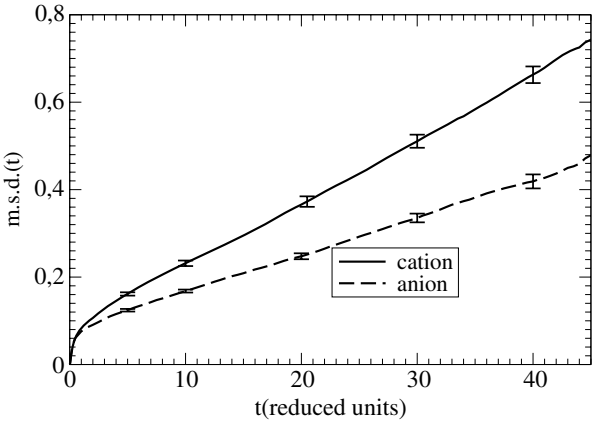

Figure 7. Mean square displacement (linear scale) of the constituents of system A for the anion (dashed line) and the cation (full line) at temperature $T = 1.0$, together with error bars.

$\tau(T) = \tau_0 \exp(\frac{-A}{T-T_0})$, the transition temperatures that are obtained are $T = 0.84$ (system B) and $T = 0.56$ (system A).

The glass transition temperature is then lowered by distributing the charge on the whole cation, which gives a smoother electrostatic potential with a smaller average well depth.

A comparison of the obtained results with experimental data is not straightforward, due to the lack of T_g data on comparable molecules and to the different methods adopted to measure them; on the basis of a comparison of data referring to imidazole and pyrrolidinium-based RTILs [30] it appears that, even if the charge delocalization consistently lowers the melting point, negligible changes are expected for the glass transition temperatures when switching from the insaturated (delocalized charge) to the saturated (localized charge) five-membered ring.

3.3. Self-diffusion behaviour

An efficient way of studying the dynamics of dense fluids is the mean square displacement (m.s.d),

$$\langle \Delta \vec{r}^2(t) \rangle = \sum_i \langle \vec{r}_i^2(t) - \vec{r}_i^2(0) \rangle \qquad (6)$$

which gives information about the mobility and thermodynamic state of the system. Figure 7 shows the linear plot of m.s.d for system A at the lowest temperature, while figure 8 reports the logarithmic plot of m.s.d. for all the three systems as the temperature is lowered from 5.0 to 1.0, well into the supposed supercooled regime. As the figure reveals, in the supercooled regime, three different regimes can be detected for all the systems studied; apart from the ballistic regime at short times ($\propto t^2$), and the diffusive regime ($\propto t^1$) at long times, the m.s.d reveals a caging regime in the time window 1–10 t (about 1–10 ps in SI time units; see section 2).

This kind of subdiffusive behaviour is peculiar to glass formers in the supercooled region [31], and has been recognized [5–8] as being given by a multiple step process. In the first step, ions are displaced by vibrations enough to disrupt

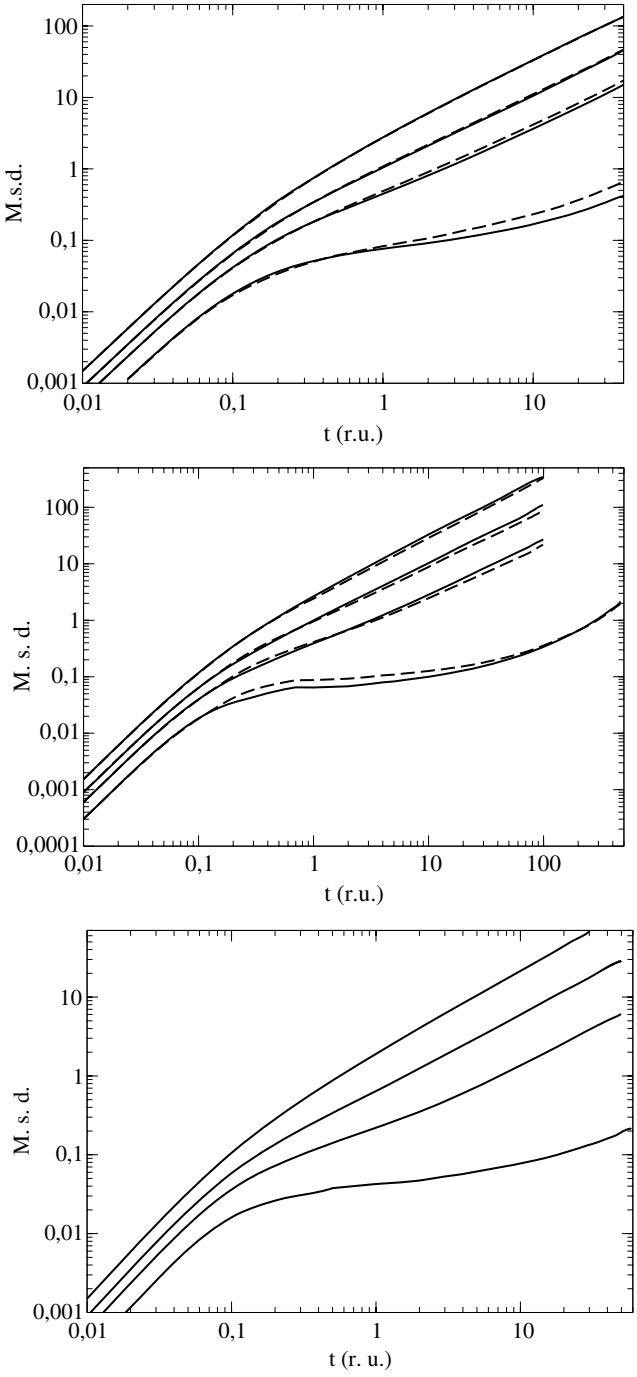

Figure 8. Mean square displacement of the constituents of system A (top), system B (middle) and system M (bottom) for the anion (full line) and the cation (dashed line) at the temperatures $T = 5.0, 3.0, 2.0, 1.0$. The anion and cation m.s.d. are coincident for system M.

a cage and form a possible escape pathway; then, an ion leaves the cage and reaches another place, where a new cage is rebuilt around it. (At high temperatures, the system switches directly from the ballistic to the diffusive regime without evidence of any caging process, due to the lower density of the melt.)

The dependence of the mean square displacement with time in ionic liquids at intermediate times has been formalized as a combination of a fast process and a slow process

Table 1. Diffusion constant for the three systems (in reduced units). The symbol (+) refers to the cation, and (−) to the anion. For systems A and B, the density is reported for each temperature followed by the symbol (ρ). In system M the diffusion constants of the oppositely charged ions coincide.

T	1.0	2.0	3.0	5.0
D_A	$0.0126 \pm 0.0011(+)$ $0.0081 \pm 0.0007(-)$ $0.661(\rho)$	$0.068 \pm 0.0051(+)$ $0.060 \pm 0.0047(-)$ $0.509(\rho)$	$0.182 \pm 0.012(+)$ $0.175 \pm 0.01(-)$ $0.414(\rho)$	$0.55 \pm 0.03(+)$ $0.55 \pm 0.03(-)$ $0.291(\rho)$
D_B	$0.0020 \pm 0.00064(+)$ $0.0025 \pm 0.0007(-)$ $0.584(\rho)$	$0.0361 \pm 0.0047(+)$ $0.0433 \pm 0.0049(-)$ $0.476(\rho)$	$0.140 \pm 0.017(+)$ $0.167 \pm 0.018(-)$ $0.394(\rho)$	$0.488 \pm 0.028(+)$ $0.573 \pm 0.031(-)$ $0.297(\rho)$
D_M	0.002 ± 0.00050	0.0206 ± 0.0066	0.0965 ± 0.012	0.338 ± 0.021

by a generalized Langevin equation [5], or as a fast cage decomposition followed by an activated hopping process [6]: in both frameworks, general semi-quantitative agreement is found between theory and numerical results. The deviation from quantitative agreement is attributed to the neglect of correlated motion in the approaches stated above.

It is noteworthy that in system A the cation, despite being larger than the anion, has greater diffusivity; this behaviour has actually been observed in RTILs by previous molecular dynamics simulations [6, 8–10] as well as in experimental studies [32]. A possible explanation has been given both in terms of the average potential energy around a cation and around an anion [10] or considering the diffusional anisotropy of the cation and anion [33]. In contrast, system B shows a different behaviour; the cation is faster than the anion in the caging regime, but becomes slower at longer times. This behaviour indicates that the distribution of charge on the whole ion, and thus the reduced depth of the potential energy wells around the cation, are responsible for the greater diffusivity of the cation in system A.

The diffusion constants calculated from the long-time part of the m.s.d. are reported in table 1; from the table, it is clear that both the symmetry breaking between cation and anion and the spreading of charge on more than one site results in a consistent increase in mobility. A comparison, even if indirect, with real ionic liquids can be performed by analysing the transport properties of saturated versus unsaturated five-membered ring compounds in bis-trifluoromethyl sulfonyl based ILs [30]: from this inspection, we note that, passing from the saturated (with more localized charge) butyl–methyl pyrrolidinium to the unsaturated (charge delocalized) butyl–methyl imidazolium, the viscosity at 298 K is lowered from 85.00 to 61.75 cP.

A further comparison can be made, noting from table 1 that the system with the delocalized charge A has faster diffusion despite its greater number density with respect to the localized charge B; this is consistent with the behaviour of the same family of RTILs already considered. The unsaturated five-membered ring butyl–methyl imidazolium has a smaller molar volume (291.17 $cm^3\ mol^{-1}$) than the saturated butyl–methyl pyrrolidinium (299.67 $cm^3\ mol^{-1}$), but nevertheless it has a lower viscosity.

Another interesting aspect is that when the temperature is lowered, system B shows a slower diffusive rate for both constituents with respect to system A.

The reduced diffusivity of system B with respect to system A can be rationalized by visualizing the diffusion process as being given by a cage-escape process typically occurring in supercooled liquids. In both systems, two kinds of cationic cages surround the anion, but with different relative populations; it is reasonable to assume that the cage given by orientational structure type number II ($\cos\theta \approx 0.33$) has got a larger opening time due to the larger contact area. Then, the preponderance of population for structure II in system B, which was shown previously, can explain why this system is slower at low temperatures, despite its larger cavity size; the transient structure in system B is found more easily in the slow-relaxing conformation with respect to system A.

Another possible suggestion that could be invoked is based on the so-called 'hole theory', which was recently used by Abbott and co-workers [34] to estimate the transport properties of molten salts and ionic liquids with a certain success. Hole theory assumes that in a fluid, which has a given distribution of cavity sizes, an ion will only be able to move if there is a cavity of suitable dimensions next to it in order to allow motion. The mobility of ion of the same dimensions should then increase with cavity size.

Different packing of the two structures leads to a different distribution of cavity size in the melt; in the more mobile liquid, the distribution should be shifted towards larger cavities. To verify this aspect, we calculated the distribution of cavity sizes with an algorithm based on a dual (Delaunay and Voronoi) tessellation of space [35] which calculates exactly the free volume of a system composed of monodisperse spheres. The results for both system A and system B at various temperatures is displayed in figure 9. The probability of having a cavity with a size large enough to accommodate a site decreases considerably with temperature. At the lowest temperature, where the liquid displays the slow subdiffusive behaviour expected for low-melting ionic liquids, the probability of having a cavity large enough to accommodate a molecule is low (about 1%), in agreement with the general consideration on low-melting ionic liquids by Abbott [34]. Nevertheless, the probability of having a cavity large enough to embed a site is actually higher in the *less* mobile system, that is, system B. The system with the narrower cavities results in the faster diffusive displacement. In addition, raising the temperature leads to a larger enhancement of cavity size for system A with respect to the cavity size displayed by system B, giving a larger average cavity size for system A at high temperatures; nonetheless, contrary to what could

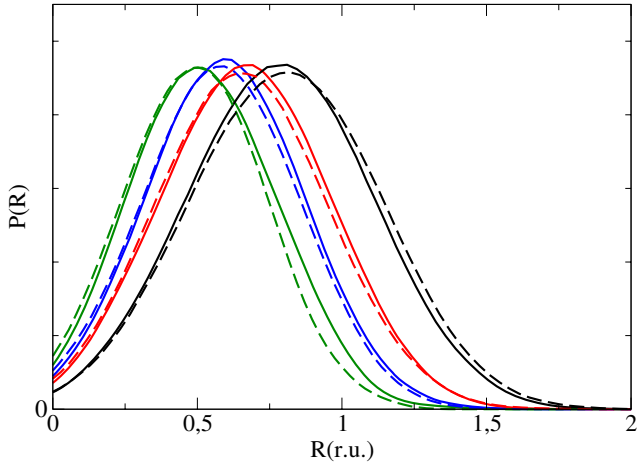

Figure 9. Probability distribution of cavity sizes for system B (full line) and system A (dashed line) at $T = 1.0$, 2.0, 3.0 and 4.0. Curves peaked at larger radii refer to growing temperatures.

be expected from hole theory, the ratio between the diffusion constant (D_A/D_B) reduces as the temperature grows.

Thus, even if hole theory can help the rationalization of the transport properties of a ionic fluid, a judgement criterion based only on cavity size distribution cannot explain the different diffusive behaviours of the two systems.

4. Conclusions

In this work, we presented a coarse-grained model for low-melting ionic liquids. The aim of this study was to verify the effect of some basic features of the molecular structure and charge distribution on the static and dynamic properties.

Our model shows typical features of RTILs in general agreement with experimental results and previous atomistic MD simulations, as the peculiar diffusional behaviour of these systems, with the bulkier and heavier cation moving faster than the anion and a correct dependence of density and transport properties on charge delocalization.

The behaviour of the order parameter distribution, of the number of neighbours in the first solvation shell, and of the diffusion suggests the existence, in the supercooled region, of stable aggregates embedded in the liquid which are progressively formed as the temperature is lowered.

A preferential ordering of pair structures appears in the liquid. A non-negligible amount of ordering begins to appear when the system is in the proximity of the liquid–solid transition (even if this point cannot be determined with absolute precision), and some ordering is detectable even in the liquid state. The contemporary presence of two possible transient structures for these liquids can explain the difference in transport properties of the systems with different charge distribution.

This analysis has been possible by defining an order parameter based on the mutual orientation of neighbouring ionic pairs. A similar definition of the order parameter (based on scalar products of vectors obtained by pair arrangement and cation and anion molecular structure) could in principle be useful for analysing the underlying structures in real ionic liquids and for unravelling the role of specific interactions (hydrogen bonding) on such structures.

In conclusion, our model is able to capture some typical aspects of the behaviour of RTILs; such simple models could be, in our view, a great help in both identifying the important molecular peculiarities of ionic liquids and investigating their general fundamental behaviour, as well as for testing new concepts to improve or modify the structural and transport properties of these materials. In future, we plan to study in detail the dynamics of these systems (as a function of temperature and pressure) and the coupling between the different kinds of motion in order to assess connections between the molecular structure and the observed deviations of ionic liquids from the ideal transport law.

Acknowledgments

This work was supported by the European Commission (EC), project FP6-(STREP), contract number 517002 (IOLISURF). Dr Giacomo Prampolini is gratefully acknowledged for helpful discussions. Professor Srikanth Sastry is gently acknowledged for providing us with the code for calculating the distribution of cavity sizes.

References

[1] Welton T and Wasserscheid P (ed) 2003 *Ionic Liquids in Synthesis* (Weinheim: Wiley–VCH)
[2] Rogers R D and Seddon K R (ed) 2003 *Ionic Liquids as Green Solvents: Progress and Prospects* (*ACS Symposium Series* vol 856) (Washington DC: American Chemical Society)
[3] Chiappe C and Pieraccini D 2005 *J. Phys. Org. Chem.* **18** 275
[4] Hanke C G, Price S L and Lynden-Bell R M 2001 *Mol. Phys.* **99** 801
[5] Margulis C J, Stern H A and Berne B J 2002 *J. Phys. Chem.* B **106** 12017
[6] Morrow T I and Maginn E J 2002 *J. Phys. Chem.* B **106** 12807
[7] Shim Y, Duan J, Choi M Y and Kim H J 2003 *J. Chem. Phys.* **119** 6411
[8] Del Popolo M G and Voth G A 2004 *J. Phys. Chem.* B **108** 1744
[9] Castro C R and Vega L F 2006 *J. Phys. Chem.* B **110** 14426
[10] Bhargava B L and Balasubramanian S 2005 *J. Chem. Phys.* **123** 144505
[11] Binder K, Baschnagel J and Paul W 2003 *Prog. Polym. Sci.* **28** 115
[12] Gay J G and Berne B J 1981 *J. Chem. Phys.* **74** 3316
[13] Gonzàlez-Melchor M, Alejandre J and Bresme F 2003 *Phys. Rev. Lett.* **90** 135506
[14] Gonzàlez-Melchor M, Bresme F and Alejandre J 2005 *J. Chem. Phys.* **122** 104710
[15] Yan Q L and de Pablo J J 2001 *Phys. Rev. Lett.* **86** 2054
[16] Bresme F, Gonzàlez-Melchor M and Alejandre J 2005 *J. Phys.: Condens. Matter* **17** S3301
[17] Wang Y and Voth G A 2006 *J. Phys. Chem.* B **110** 18601
[18] Hunt P A and Gould I R 2006 *J. Phys. Chem.* A **110** 2269
[19] Tsuzuki S, Tokuda H, Hayamizu K and Watanabe M 2005 *J. Phys. Chem.* B **109** 16474
[20] Israelachvili J N 1998 *Intermolecular and Surface Forces* (London: Academic)
[21] Hu Z H and Margulis C J 2006 *Proc. Natl Acad. Sci.* **103** 831
[22] Wang Y T and Voth G A 2005 *J. Am. Chem. Soc.* **127** 12192
[23] Errington J R and DeBenedetti P G 2001 *Nature* **409** 318

[24] Kanakubo M, Harris R K, Tsuchihashi N, Ibuki K and Ueno M 2007 *J. Phys. Chem.* B **111** 2062
[25] Aoyagi T, Takimoto J and Doi M 2001 *J. Chem. Phys.* **115** 552 Visit also http://www.octa.jp.
[26] Pàdua A A H and Canongia Lopes J N 2006 *J. Phys. Chem.* B **110** 3330
[27] Stanley H E, Buldyrev S, Franzese G, Giovambattista N and Starr F W 2005 *Phil. Trans. R. Soc.* A **363** 509
[28] Wendt H R and Abraham F F 1978 *Phys. Rev. Lett.* **41** 1244
[29] Shim Y, Choi M Y and Kim H J 2005 *J. Chem. Phys.* **122** 044511
[30] Zhang S, Sun N, He X, Lu X and Zhang X 2006 *J. Phys. Chem. Ref. Data* **35** 1475
[31] Donth E 2001 *The Glass Transition* (Berlin: Springer)
[32] Umecky T, Kanakubo M and Ikushima Y 2005 *Fluid Phase Equilib.* **329** 228
[33] Urahata S M and Ribeiro M C C 2005 *J. Chem. Phys.* **122** 24511
[34] Abbott A P 2004 *ChemPhysChem* **5** 1242
[35] Sastry S, Corti D S, Debenedetti P G and Stillinger F H 1997 *Phys. Rev.* E **56** 5524